

# Flow to strong coupling in the two-dimensional Hubbard model

Carsten Honerkamp<sup>1a</sup>, Manfred Salmhofer<sup>2</sup>, and T.M. Rice<sup>1</sup>

<sup>1</sup> Theoretische Physik, ETH-Hönggerberg, CH-8093 Zürich, Switzerland

<sup>2</sup> Theoretische Physik, Universität Leipzig, D-04109 Leipzig, Germany

March 13, 2002

**Abstract.** We extend the analysis of the renormalization group flow in the two-dimensional Hubbard model close to half-filling using the recently developed temperature flow formalism. We investigate the interplay of  $d$ -density wave and Fermi surface deformation tendencies with those towards  $d$ -wave pairing and antiferromagnetism. For a ratio of next nearest to nearest neighbor hoppings,  $t'/t = -0.25$ , and band fillings where the Fermi surface is inside the Umklapp surface, only the  $d$ -pairing susceptibility diverges at low temperatures. When the Fermi surface intersects the Umklapp surface close to the saddle points,  $d$ -wave pairing,  $d$ -density wave, antiferromagnetic and, to a weaker extent,  $d$ -wave Fermi surface deformation susceptibilities grow together when the interactions flow to strong coupling. We interpret these findings as indications for a non-trivial strongly coupled phase with short-ranged superconducting and antiferromagnetic correlations, in close analogy with the spin liquid ground state in the well-understood two-leg Hubbard ladder.

**PACS.** 71.10.Fd Lattice fermion models (Hubbard model, etc.) – 74.72.-h High-Tc compounds

## 1 Introduction

The two-dimensional (2D) Hubbard model is a focus of electron correlation theory because of its relevance to high-temperature superconductivity [1] and other correlation phenomena such as metal-insulator transitions [2] and itinerant ferromagnetism [3]. Apart from proposed exotic spin-liquid or non-Fermi liquid states [1, 4, 5] a widely adopted approach is to classify possible ground states of the model in terms of broken symmetries. This can be done for the strong-coupling versions of the Hubbard model by invoking spin-charge separation [6] or large-spin approaches [7]. But for moderate interaction strengths it is more common to invoke a mean field description of long-range ordered ground states with anomalous expectation values which are bilinear in electron creation and annihilation operators. These theories are either constructed with the bare Hubbard interaction [8, 9] or with an effective interaction which is postulated or calculated perturbatively, e.g. by one-loop renormalization group (RG) treatments or parquet summations. Typically these treatments are restricted to the weakly correlated case, but often they can give qualitatively satisfactory results such as the antiferromagnetic state at half-filling or a  $d_{x^2-y^2}$ -superconducting ground state at a reduced band filling in the 2D Hubbard model [10, 11, 12, 13, 14].

Recently two independent proposals enlarging the variety of potential symmetry-broken states have been made. One possibility was raised by Halboth and Metzner [11], based on an analysis of the Landau function extracted from a RG flow. They pointed out that the system might become unstable against a Pomeranchuk instability, i.e. a spontaneous deformation of the Fermi Surface (FS) reducing its symmetry from square to orthorhombic. Qualitatively similar results were obtained by Valenzuela and Vozmediano [15] in a mean-field study of an extended Hubbard model. However with this technique and also with the Wilsonian RG formalism based on an infrared (IR) cutoff used in Ref. [11] it is difficult to compare the strength of the FS deformation tendencies with other potential singularities, e.g. in the AF or  $d$ -wave superconducting channel. Here we use the recently developed temperature-flow formalism [16], to analyze these FS deformation tendencies together with other channels in an unbiased way.

A different type of symmetry breaking was considered by Nayak [17] and Chakravarty et al. [18]. They proposed that a  $d$ -density-wave state (closely related to flux phases [19] or orbital antiferromagnets [20]) forms at a high temperature in the underdoped high- $T_c$  cuprates and is responsible for the many anomalous properties like the notorious pseudogap. This proposal has been controversial for a number of reasons [21, 22], not least because of the absence of experimental evidence that the onset of the pseudogap is accompanied by an actual phase transition rather than a continuous crossover. The onset of a phase with broken translational and time reversal symme-

<sup>a</sup> New address: Department of Physics, Massachusetts Institute of Technology, Cambridge MA 02139, USA, e-mail: carsten@mit.edu

tries should cause anomalies in thermodynamic and other properties which have not been observed. Nonetheless it is interesting to investigate whether  $d$ -density-wave tendencies play a significant role in the RG flow to strong coupling.

In this paper we show that in the one-loop RG temperature-flow to strong coupling in the  $t$ - $t'$  Hubbard model at  $U \approx 3t$  both the FS deformation and  $d$ -density wave tendencies grow. However their growth is weaker than that of  $d$ -wave pairing and AF fluctuations, so that they do not appear as the dominant instabilities of the model. Nonetheless, similar to our findings with a RG IR-flow in Ref. [12], we find a particular density region - the so-called *saddle-point regime* which occurs when the FS is close to the saddle points of the band dispersion at  $(\pi, 0)$  and  $(0, \pi)$  - where  $d$ -wave pairing, AF,  $d$ -density wave and  $d$ -wave Pomeranchuk fluctuations are intimately related and grow together in the range where the one-loop flow is credible. This contrasts with the behavior for fillings smaller than the van Hove filling where only the  $d$ -wave pairing correlations continue to grow towards lower temperatures, while the others are cut off below some temperature.

The qualitative picture obtained here is a confirmation and extension of the results described in Ref. [12]. The main motivation for the present paper is twofold: *a*) we show that the new temperature-flow RG scheme reproduces the results of the IR-flow RG [12] and yields an even clearer picture; *b*) we now also include  $d$ -wave FS deformations and  $d$ -density wave tendencies which were not considered in the previous analysis.

In the following we first describe the calculational scheme and the symmetry-breaking tendencies which are investigated. Then we discuss our numerical results for the case of zero and non-zero values of the next-nearest hopping  $t'$  and conclude with a comparison of our observations to ladder systems, which we argue give some insights into the nature of the strongly coupled state.

## 2 The calculational scheme

The Hamiltonian for the 2D  $t$ - $t'$  Hubbard model is

$$H = -t \sum_{\text{n.n.}, s} c_{i,s}^\dagger c_{j,s} - t' \sum_{\text{n.n.n.}, s} c_{i,s}^\dagger c_{j,s} + U \sum_i n_{i\uparrow} n_{i\downarrow}$$

with onsite repulsion  $U$  and hopping amplitudes  $t$  and  $t'$  between nearest neighbors (n.n.) and next-nearest neighbors (n.n.n.) on the 2D square lattice. We apply the so-called temperature-flow RG scheme introduced recently [16] in a  $N$ -patch implementation that covers the full Fermi surface. Similar to the approaches in Refs. [10, 11, 12, 23] the  $T$ -flow scheme is derived from an exact RG equation. However, a low energy IR cutoff is not used, and instead the temperature  $T$  itself is used as the flow parameter. This new formulation allows an unbiased comparison between AF and FM tendencies, whereas RG schemes with a flowing IR cutoff artificially suppress particle-hole excitations with small wave vectors, e.g. long wavelength density fluctuations. For a detailed discussion of this matter

and a derivation of the  $T$ -flow RG equations the reader is referred to Ref. [16].

The RG formalism yields a hierarchy of differential equations for the one-particle irreducible  $n$ -point vertex functions,  $\Gamma_T^{(n)}$ , as functions of the temperature. Integration of this system of equations gives the temperature-flow. As initial condition we assume that at a high temperature  $T_0$ , the single-particle Green's function of the system is simply  $G_0(i\omega, \mathbf{k}) = [i\omega - \epsilon(\mathbf{k})]^{-1}$  and the interaction vertex is given by a local repulsion,  $U$ . This is justified if  $T_0$  is sufficiently large, as wavevector-dependent perturbative corrections to selfenergy and four-point vertex decay at least  $\propto 1/T_0^1$ . We truncate the infinite system of equations by dropping all vertex functions  $\Gamma_T^{(n)}$  with  $n > 4$ . In the present treatment we also neglect selfenergy corrections and the frequency dependence of the vertex functions. This restricts the scheme to one-loop equations for the spin-rotation invariant four-point vertex  $\Gamma_T^{(4)}$ . Starting with weak to moderate interactions, we follow the  $T$ -flow of  $\Gamma_T^{(4)}$  as  $T$  decreases.

The four-point vertex  $\Gamma_T^{(4)}$  is determined by a coupling function  $V_T(\mathbf{k}_1, \mathbf{k}_2, \mathbf{k}_3)$  (see Refs. [12, 16, 23]). The numerical implementation follows the work of Zanchi and Schulz [10] and was already explained in Refs. [12] and [16]. We define elongated phase space patches around lines leading from the origin of the BZ to the  $(\pm\pi, \pm\pi)$ -points, and approximate  $V_T(\mathbf{k}_1, \mathbf{k}_2, \mathbf{k}_3)$  by a constant for all wave vectors in the same patch. We calculate the RG flow for the discrete subset of interaction vertices with each FS patch represented by a single wave vector and with the initial condition  $V_{T_0}(\mathbf{k}_1, \mathbf{k}_2, \mathbf{k}_3) \equiv U$ . Most calculations were performed using 48 patches. Furthermore we calculate the flow of several static susceptibilities, as described below. In addition we consider the flow of the couplings  $h_c(\mathbf{k})$  of quasiparticles at different positions on the Fermi surface to uniform static charge fields. This allows us to analyze which classes of coupling functions and which susceptibilities become important at low  $T$ . For a large parameter range, we observe a flow to strong coupling, i.e. at sufficiently low temperature some components of the coupling function  $V_T(\mathbf{k}_1, \mathbf{k}_2, \mathbf{k}_3)$  become larger than the bandwidth. The approximations mentioned above fail when the couplings are too large. Therefore we stop the flow when the largest coupling exceeds a high value larger than the bandwidth, e.g.  $V_{T,\text{max}} = 18t$ . This defines a *characteristic temperature*  $T^*$  of the flow to strong coupling.

## 3 Antiferromagnetic, $d$ -wave pairing, $d$ -density waves and $d$ -wave Pomeranchuk fluctuations

In this section we introduce fermionic coupling terms to order parameters or static external fields corresponding

<sup>1</sup> A wavevector-independent contribution can be absorbed into the chemical potential  $\mu$ . Flows with fixed particle number instead of fixed  $\mu$  give qualitatively similar results.

to different symmetry breaking channels. Within the RG treatment described in the previous section, we then calculate the one-loop renormalizations of these coupling terms and thus obtain information on the growth of the corresponding fluctuations in the low-temperature state. A divergence of one of these external couplings signals a crossover to a region with a strong tendency to ordering which could become an actual finite temperature phase transition when coupling in a third spatial direction is added.

First we introduce the  $d$ -wave pairing field  $\Phi_{s,d-sc} = -\Phi_{-s,d-sc}$ , which couples to the electrons via

$$\Phi_{s,d-sc} \sum_{\mathbf{k}} h_{d-sc}(\mathbf{k}) c_{\mathbf{k},s}^\dagger c_{-\mathbf{k},-s}^\dagger. \quad (1)$$

with a coupling constant  $h_{d-sc}(\mathbf{k})$ . As initial condition at  $T = T_0$  we assume a  $d_{x^2-y^2}$  form factor  $h_{d-sc}(\mathbf{k}) = (\cos k_x - \cos k_y) / \sqrt{2}$ . Like the other coupling constants defined below,  $h_{d-sc}$  will develop a  $\mathbf{k}$ -dependence through the perturbative corrections in the course of the temperature flow towards lower  $T$  and higher harmonics of the same representation of the point group will be admixed. Next we also define a ( $s$ -wave) spin-density wave field  $\Phi_{AF}$ . Due to spin-rotational invariance it is sufficient to consider staggered fields in the spin quantization direction,

$$\Phi_{z,AF} \sum_{\mathbf{k}} h_{AF}(\mathbf{k}) \left( c_{\mathbf{k}+\mathbf{Q},s}^\dagger c_{\mathbf{k},s} - c_{\mathbf{k}+\mathbf{Q},-s}^\dagger c_{\mathbf{k},-s} \right). \quad (2)$$

Here the momentum transfer  $\mathbf{Q} = (\pi, \pi)$  between created and annihilated particles corresponds to an alternating field acting on the electron spins on n.n. sites. The initial condition at high temperatures is  $h_{AF}(\mathbf{k}) = 1$ . The proposed Pomeranchuk deformations also have  $d_{x^2-y^2}$  symmetry, the coupling term is given by

$$\lim_{\mathbf{q} \rightarrow 0} \Phi_{d-P} \sum_{\mathbf{k},s} h_{d-P}(\mathbf{k}) c_{\mathbf{k}+\mathbf{q},s}^\dagger c_{\mathbf{k},s}^\dagger, \quad (3)$$

with initial condition  $h_{d-P}(\mathbf{k}) = (\cos k_x - \cos k_y) / \sqrt{2}$  at  $T_0$ . A non-zero  $d$ -wave Pomeranchuk field  $\Phi_{d-P}$  lifts the degeneracy of the saddle points at  $(\pi, 0)$  and  $(0, \pi)$  and breaks the fourfold symmetry of the kinetic energy. The  $d$ -density wave fluctuations couple to particle-hole pairs with momentum transfer  $\mathbf{Q}$ ,

$$\Phi_{d-DW} \sum_{\mathbf{k},s} h_{d-dw}(\mathbf{k}) c_{\mathbf{k}+\mathbf{Q},s}^\dagger c_{\mathbf{k},s} \quad (4)$$

with initial conditions chosen as

$$h_{d-DW}(\mathbf{k}) = (\cos k_x - \cos k_y) / \sqrt{2}$$

at the initial temperature  $T_0$ . In the one-loop  $T$ -flow RG treatment [16, 23] the coupling constants  $h$  are then renormalized according to

$$\frac{d}{dT} h_{d-sc}(\mathbf{k}) = -\frac{1}{N_L} \sum_{\mathbf{k}'} h_{d-sc}(\mathbf{k}') V_T(\mathbf{k}, -\mathbf{k}, \mathbf{k}')$$

$$\cdot \frac{d}{dT} L_{PP}(\mathbf{k}', -\mathbf{k}'), \quad (5)$$

$$\frac{d}{dT} h_{AF}(\mathbf{k}) = -\frac{1}{N_L} \sum_{\mathbf{k}'} h_{AF}(\mathbf{k}') V_T(\mathbf{k}, \mathbf{k}', \mathbf{k} + \mathbf{Q}) \cdot \frac{d}{dT} L_{PH}(\mathbf{k}', \mathbf{k}' + \mathbf{Q}), \quad (6)$$

$$\frac{d}{dT} h_{d-DW}(\mathbf{k}) = -\frac{1}{N_L} \sum_{\mathbf{k}'} h_{d-DW}(\mathbf{k}') \frac{d}{dT} L_{PH}(\mathbf{k}', \mathbf{k}' - \mathbf{Q}) \cdot [V_T(\mathbf{k}, \mathbf{k}', \mathbf{k}' + \mathbf{Q}) - 2V_T(\mathbf{k}, \mathbf{k}', \mathbf{k} + \mathbf{Q})], \quad (7)$$

$$\frac{d}{dT} h_{d-P}(\mathbf{k}) = -\frac{1}{N_L} \sum_{\mathbf{k}'} h_{d-P}(\mathbf{k}') \frac{d}{dT} L_{PH}(\mathbf{k}', \mathbf{k}') \cdot [V_T(\mathbf{k}, \mathbf{k}', \mathbf{k}') - 2V_T(\mathbf{k}, \mathbf{k}', \mathbf{k})]. \quad (8)$$

The expressions on the right hand side are evaluated in absence of the external fields.  $N_L$  denotes the number of lattice sites and the particle-particle and particle-hole loops are given by

$$L_{PP}(\mathbf{k}, \mathbf{k}') = T \sum_{i\omega_n} \frac{1}{i\omega_n - \epsilon_{\mathbf{k}}} \frac{1}{-i\omega_n - \epsilon_{\mathbf{k}'}}$$

and

$$L_{PH}(\mathbf{k}, \mathbf{k}') = T \sum_{i\omega_n} \frac{1}{i\omega_n - \epsilon_{\mathbf{k}}} \frac{1}{i\omega_n - \epsilon_{\mathbf{k}'}}$$

where  $i\omega_n$  denotes the fermionic Matsubara frequencies  $\omega_n = \pi T(2n + 1)$  with  $n = 1, 2, \dots$ . The susceptibilities for the various channels are also renormalized by temperature derivatives of bubble diagrams with the corresponding couplings at the vertices. For example for the  $d$ -wave pairing susceptibility we obtain

$$\frac{d}{dT} \chi_{d-sc} = \frac{1}{N_L} \sum_{\mathbf{k}} h_{d-sc}(\mathbf{k}) \cdot \frac{d}{dT} L_{PP}(\mathbf{k}, -\mathbf{k}) h_{d-sc}(-\mathbf{k}). \quad (9)$$

Analogous expressions hold for the other susceptibilities. As initial condition we assume that all susceptibilities are zero at the initial high temperature,  $T_0$ .

## 4 Results for the 2D Hubbard model

Here we describe our numerical results obtained with the  $N$ -patch implementation of the one-loop  $T$ -flow RG scheme with  $N = 48$  patches. For all cases discussed below, the RG flow goes to strong coupling. This means that some components of the coupling function become larger than the perturbative range when the temperature is lowered far enough. We define a characteristic temperature  $T^*$  for the flow to strong coupling determined as the temperature when the largest coupling reaches  $V_{\max} = 18t$ .

#### 4.1 The case $t' = 0$

First let us discuss results for vanishing next-nearest neighbor hopping,  $t' = 0$ . The flow of the susceptibilities is summarized in Fig. 1.

For the square Fermi surface at half band filling, i.e.  $\mu = 0$ , we find that the AF susceptibility is the leading divergent susceptibility, consistent with the expected AF ordered ground state. We also find weaker growing  $d$ -wave pairing and  $d$ -density wave susceptibilities. At  $\mu = 0$ , these two channels have exactly the same temperature dependence due to the particle-hole symmetry;  $\epsilon(\mathbf{k}) = -\epsilon(\mathbf{k} + \mathbf{Q})$ . For finite doping, i.e.  $\mu \neq 0$ , the flow splits this degeneracy and the  $d$ -wave pairing generally grows more strongly than the  $d$ -density wave channel. As the electron density is further reduced below half-filling, the nesting in the  $(\pi, \pi)$  particle-hole channel is increasingly weakened. Correspondingly, at a critical doping that depends on the interaction strength, the growth in the AF and  $d$ -density wave channels get cut off at low  $T$  and the  $d$ -wave pairing is the only divergent channel that remains. This crossover from the AF dominated flow to the  $d$ -wave pairing dominated instability for  $t' = 0$  is very similar to the results of Zanchi and Schulz [10] and Halboth and Metzner [11] who used a  $N$ -patch scheme with flowing IR cutoff. Within the latter schemes it is difficult to compare the flow of small- $\mathbf{q}$  particle-hole susceptibilities, e.g. Pomeranchuk FS deformations, with the flow of AF or superconducting susceptibilities. There is no such difficulty in the temperature flow scheme. Thus we can directly compare the Pomeranchuk channel with the above-mentioned other tendencies. The main conclusion arising from the data shown in Fig. 1 is that the  $d$ -wave Pomeranchuk tendencies grow somewhat to lower temperatures, but apparently they do not represent the leading instability for the  $t' = 0$  Hubbard model with only a local onsite repulsion as in initial interaction. In this paper we do not give a systematic analysis how the leading instability may change when the initial interaction is varied, e.g. by including a n.n.n. repulsion  $V$  or a spin exchange coupling  $J$ . This question was addressed by Binz et al. [26] for the half-filled case and  $U \rightarrow 0$ . These authors found a  $d$ -density wave regime for sufficiently large positive n.n. Heisenberg coupling  $J$  between an AF regime at small n.n. repulsion  $V$  and  $s$ -charge density wave regime at  $4V > U$ . We find a similar crossover between the two latter regimes for  $U \geq 0.3t$ . However a RG flow where the  $d$ -density wave susceptibility grows most strongly was only found for a limited parameter region around  $J \geq 0.7U$  and  $4V \approx 0.7U$ .

#### 4.2 Moderate n.n.n. hopping $t' = -0.25t$

Next we focus on the case of n.n.n. neighbor hopping  $t' = -0.25t$  and band fillings  $n < 1$  for which the FS passes close to the saddle points. Upon increasing the particle density through the van Hove filling at which  $\mu$  lies exactly at the van Hove singularity, i.e.  $\mu = 4t'$ , the FS starts to intersect the Umklapp surface which connects the  $(\pi, 0)$  and  $(0, \pi)$  points with straight lines. As we will

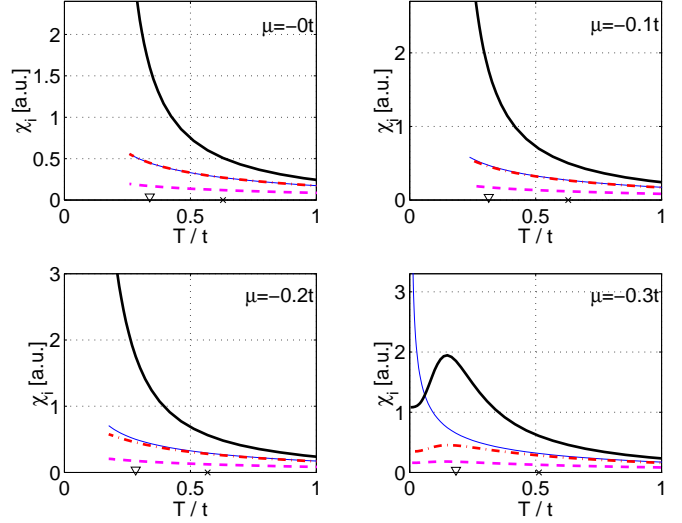


**Fig. 1.** Temperature flow of AF (thick solid line),  $d$ -wave  $sc$  pairing (thin solid line),  $d$ -density wave (dashed-dotted line) and  $d$ -Pomeranchuk susceptibilities for different values of the chemical potential and  $t' = 0$ . The cross and the triangle at the  $T$  axis denote the temperatures where the largest couplings exceed  $5t$  and  $10t$ . Half filling corresponds to  $\mu = 0$ .

show, this gives rise to a remarkable qualitative change in the flow. Two typical shapes of the non-interacting Fermi surfaces for densities below and above the van Hove filling are shown in Fig. 2.

In Fig. 3 we show the evolution of  $d$ -wave pairing, AF,  $d$ -density wave and  $d$ -wave Pomeranchuk susceptibilities for different values of the chemical potential as the temperature is lowered. In the first upper two plots for which  $\mu < 4t'$ , we observe that only the  $d$ -wave pairing susceptibility grows rapidly at low temperatures  $T \rightarrow T^* > 0$ . The other susceptibilities reach a maximum at a  $T_{\max} > T^*$  and decrease again as  $T \rightarrow T^*$ . For the next two plots the FS intersects the Umklapp surface close to the saddle points and the flow is qualitatively different: now all four susceptibilities grow as  $T \rightarrow T^*$ . As described in Ref. [12], the flows of AF and  $d$ -wave pairing susceptibilities are very similar for a broad density region above the saddle point filling and it appears to be implausible that the strong coupling state is a simple symmetry-broken state corresponding to a single type of ordering. More than that, the  $d$ -density wave and  $d$ -wave Pomeranchuk susceptibilities also grow as  $T \rightarrow T^*$ . But for our parameters these two channels do not constitute the leading instabilities. Nevertheless they seem to be part of a common mechanism arising from the special location of the FS close to saddle points which causes mutual reinforcement of different channels, most prominently AF and  $d$ -wave pairing described in Ref. [12]. The main reason for this effect is that the scattering processes connecting the two inequivalent saddle point regions involve particle pairs with small total momentum that scatter with wavevector transfers close to  $(\pi, \pi)$ . Therefore these scattering processes are strongly driven by both the Cooper and the  $(\pi, \pi)$  particle-

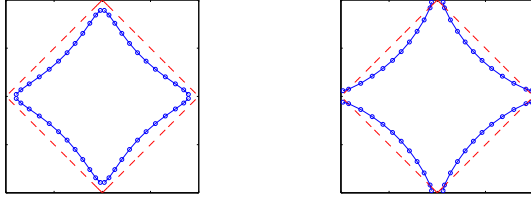


**Fig. 2.** Non-interacting Fermi surfaces with  $t' = -0.25t$  for  $\mu = -1.05t$  (left plot,  $\langle n \rangle \approx 0.75$  per site) and  $\mu = -0.95t$  (right plot,  $\langle n \rangle \approx 0.82$  per site). The dots denote the location of the 48 points for which the flow of the coupling function is evaluated. The dashed square denotes the so-called Umklapp surface.

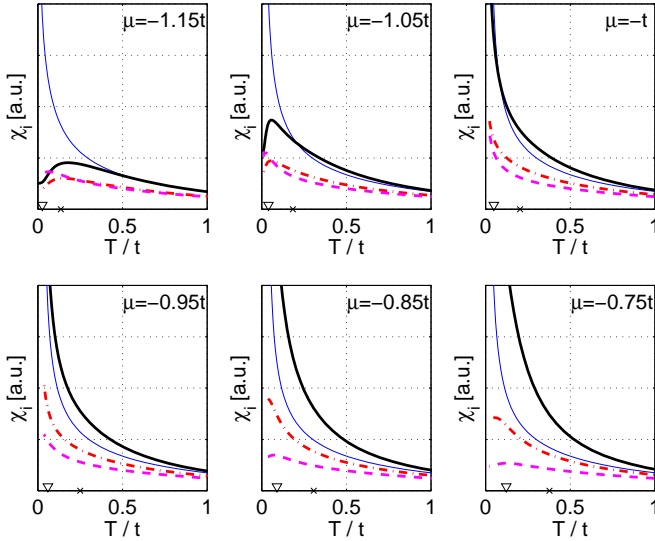


**Fig. 3.** Temperature flow of AF (thin solid line),  $d$ -wave pairing (thick solid line),  $d$ -density wave (dashed-dotted line) and  $d$ -Pomeranchuk susceptibilities for different values of the chemical potential and  $t' = -0.25t$ . The cross and the triangle at the  $T$  axis denote the temperatures where the largest couplings exceed  $5t$  and  $10t$ . Band fillings less than the saddle point filling correspond to  $\mu < -t$ .  $\langle n \rangle \approx 0.93$  per site for  $\mu = -0.75t$ .

hole channel and this causes a mutual reinforcement of the fluctuations generated by these channels. Thus it is interesting to speculate that the strong coupling state will embody all these channels as short range correlations, instead of selecting a single ordering channel and suppressing the others. Indeed, as discussed in the concluding section, examples for such ground states are known from ladder systems. Furthermore, other numerical investigations of the doped 2D  $t$ - $J$  model showed the existence of  $d$ -density wave correlations in Gutzwiller-projected  $d$ -wave pairing variational wave-functions [24] and in the lowest energy  $d$ -wave paired states in exact diagonalization on a 32-site cluster [25].

We note that if we continue to follow the one-loop RG flow for the 2D system which ignores selfenergy corrections, the common growth of the different channels

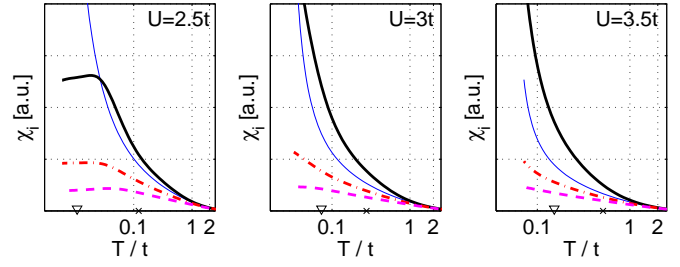


**Fig. 4.** Temperature flow of AF (thin solid line),  $d$ -wave pairing (thick solid line),  $d$ -density wave (dashed-dotted line) and  $d$ -Pomeranchuk susceptibilities for different values of the initial interaction  $U$  and  $\mu = -0.92t$  at  $t' = -0.25t$ . The cross and the triangle at the  $T$  axis denote again the temperatures where the largest couplings exceed  $5t$  and  $10t$ .

does not continue to arbitrarily low temperatures. Typically a decoupling takes place once the overlap between the channels becomes too small due to the restriction of the relevant scattering processes at low temperatures to thinner and thinner neighborhoods of the Fermi surface. Signs for this are visible for example in the flow of  $d$ -density wave susceptibility in the last plot of Fig. 3. However we are convinced that one should concentrate on the flow down to temperatures where the growing interactions reach values comparable to the bandwidth. This is also the scale where the corrections to the one-loop RG equations such as one- and two-loop selfenergy effects start to become non-negligible [12,13]. In the saddle point regime described above the decoupling of the different channels only occurs at lower temperatures where the one-loop flow without selfenergy corrections has lost its validity as the couplings are much larger than the bandwidth. Obviously, the density range where this common flow of several channels occurs becomes larger with increasing interaction strengths  $U$ . The reason is that at higher temperature scales a wider shell around the FS participates in the RG flow and the overlaps between the scattering processes driving the individual fluctuations are larger. This is illustrated in Fig. 4, where we plot the flow of the susceptibilities for the same chemical potential but for different initial interactions  $U$ . While for  $U = 2.5t$  the flows of AF,  $d$ -density wave and  $d$ -wave Pomeranchuk susceptibilities go through a maximum before the couplings exceed the bandwidth, for  $U \geq 3t$  their flow grows monotonically over the range where the one-loop flow applies. Thus we expect that there is a nonzero minimal interaction strength above which the coupled saddle point flow determines the ground state properties. For smaller interactions the low energy physics may be dominated by a single channel.

With the new  $T$ -flow RG scheme we again find an anisotropic suppression of the charge compressibility in the saddle point regime, similar to our findings in Ref. [12]. This is illustrated in Fig. 5, where we plot the  $T$ -flow of the couplings to external static uniform charge fields,  $h_c(\mathbf{k})$ . These quantities are calculated in a way analogous to the Pomeranchuk coupling constants  $h_{d-P}(\mathbf{k})$ , with the differ-

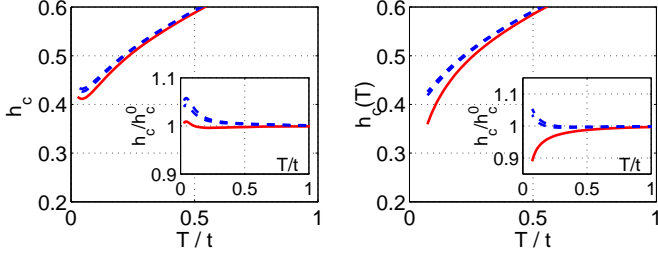


**Fig. 5.** Temperature flow of couplings  $h_c(\mathbf{k}_F)$  of quasiparticles on different points  $\mathbf{k}_F$  on the FS to uniform static charge fields. The insets show the flow normalized to the RPA values for the corresponding temperatures. The solid (dashed) lines correspond to  $\mathbf{k}_F$  points close to the saddle points (BZ diagonals). The left plot is for  $\mu = -1.1t$  (band filling less than the van Hove value,  $d$ -wave regime, band filling less than van Hove filling), and the right plot for  $\mu = -0.95t$  (saddle point regime, band filling slightly larger than van Hove filling).

ence that the  $d$ -wave form factor in Eq. (3) is replaced by unity. In the left plot the density is less than the van Hove filling corresponding to the pure  $d$ -wave regime and the charge couplings  $h_c(\mathbf{k})$  are suppressed uniformly around the FS. Moreover, as shown in the inset, the RG flow of the interactions enhances the charge couplings  $h_c(\mathbf{k})$  with respect to isotropic RPA (random phase approximation) values  $h_c^0$  calculated without RG flow of the interactions. In the right plot, we show the same quantities for  $\mu = -0.95t$ , corresponding to the saddle point regime at band fillings slightly larger than the van Hove value. Here the suppression of the charge couplings is strongest in the FS region close to the saddle points. Furthermore, compared to the RPA values, the charge couplings for this FS region are strongly decreased at low  $T$  by the RG flow of the interactions, while they increase near to the BZ diagonals. We emphasize that these tendencies are rather weak because we do not let the interactions become too strong. Nevertheless, our findings with the new  $T$ -flow RG scheme are again consistent with the hypothesis of a Fermi surface truncation [27,12] at the saddle points where the scattering processes grow most strongly, with remaining FS arcs around the BZ diagonals. We believe that the effects observed as tendencies in the weak-coupling approach will be strongly amplified in a full strong coupling description. We add that a similar suppression of the  $\mathbf{k}$ -space resolved compressibility at the saddle points is observed within a Landau-Fermi liquid framework [28] and was also found in quantum Monte Carlo calculations for the half filled Hubbard model by Otsuka et al. [29].

Lastly we comment on the behavior of the  $T$ -flow RG scheme as the density is increased towards half filling. The saddle points move to larger negative band energies and the coupling between the channels becomes less effective (see middle and right lower plots in Fig. 3). The AF susceptibility grows most strongly at higher  $T$ . At lower temperatures the  $T$ -flow RG scheme exhibits a stronger sensitivity to the imperfect nesting introduced by the n.n.n. hopping term  $t'$  than in the IR-flow RG scheme we used

previously [12]. This shows up in a saturation of the AF susceptibility flow for weaker initial interactions at low  $T$  before the couplings have reached values larger than the bandwidth. At half-filling an initial value of  $U \geq 3.5t$  is required to obtain the dominant AF phase found in Ref. [12].

## 5 Conclusions and comparison with the two-leg Hubbard ladder

We have investigated the flow of  $d$ -wave pairing, spin density wave,  $d$ -density wave and  $d$ -wave Pomeranchuk susceptibilities in the two-dimensional Hubbard model near the van Hove filling. For a n.n.n. hopping  $t' = -0.25t$  we found two distinct regimes. For densities well away from the van Hove density, only a single susceptibility diverges at low  $T$ . For a range of band fillings  $n < 1$  around, or somewhat above, the van Hove filling, whose width depends on the strength of the initial interaction, several susceptibilities grow together when the interactions flow to strong coupling. In particular, from the interplay between  $d$ -wave pairing and AF tendencies near the saddle points, also described in Ref. [12], we conclude that the strong coupling phase, in the saddle point regions, is not given by a dominance of a single ordering such as superconducting, magnetic or charge ordering. Furthermore we again find tendencies towards incompressibility of the FS Pomeranchuk regions near the saddle points which can be interpreted as indication for a FS truncation. Although the  $d$ -density wave and  $d$ -wave FS deformation modes get enhanced at lower temperatures, but do not represent the leading instabilities for the  $t$ - $t'$  Hubbard model with weak to moderate repulsive onsite interaction. This renders a spontaneous symmetry breaking in these channels unlikely. Nevertheless there may be significant short ranged correlations of the respective types.

A similar RG flow to strong coupling is also found in the half-filled two-leg Hubbard ladder. This quasi-one-dimensional system has been extensively analyzed both from the weak-coupling perspective [30,31,32] and by numerical methods for stronger onsite repulsion [33]. Through these studies it became clear that the ground state for all  $U$  is given by an *insulating spin liquid*, i.e. spin and charge fluctuations are gapful and decay exponentially. The FS is fully truncated although no symmetry breaking occurs.

The weak-coupling analysis [30,31] typically starts with a one-loop RG scheme which selects the relevant couplings. Subsequently the effective Hamiltonian, composed of the kinetic energy and the relevant couplings, is bosonized and the properties of spin and charge excitations can be deduced. Our comparison with the 2D Hubbard model focuses on only this one-loop RG step. In the one-loop g-ology for the half-filled two-leg ladder, one finds seven relevant coupling constants  $g_i$ ,  $i = 1, \dots, 7$  which describe scattering processes between the 4 Fermi points, 2 in the even parity band and 2 in the odd band. In the RG flow with decreasing infrared cut-off  $\Lambda$  and initial condition  $g_i(\Lambda_0) = U$  these coupling constants diverge asymptoti-



cally together as

$$g_i(\Lambda) = \frac{g_i^0}{\log(\Lambda/\Lambda_c)}, \quad (10)$$

when  $\Lambda$  is reduced towards a finite critical scale  $\Lambda_c$ . The  $g_i^0$  reach fixed ratios in the weak interaction limit. Due to the divergence of the coupling functions, the one-loop renormalizations drive several couplings to external fields to infinity. Like in the 2D system several types of fluctuations are driven by common scattering processes and mutually reinforce each other. As mentioned in the last section, in the 2D model we need a finite initial interaction strength  $U$  to observe the coupled flow of several channels for a reasonably wide parameter region. In contrast with that in the two-leg ladder the mutual reinforcement is present at all energy scales and occurs for arbitrarily weak interactions. More precisely, with the asymptotic flow given by Eq. (10) we find that in the half-filled ladder AF,  $d$ -wave pairing,  $d$ -density wave and spin density wave couplings grow with the same strength<sup>2</sup>. Equivalently, if we write down the effective Hamiltonian of the system close to the critical scale, the effective coupling constants for mean-field decouplings in  $d$ -wave pairing, AF and  $d$ -density wave channel reach the same absolute value in the asymptotic flow very close to the instability. Since the effective densities of states for the three types of mean-field decouplings are the same, their potential ground state energies are degenerate as well. Nonetheless, as we know from the bosonization [31] and numerical studies [33], the ground state does not exhibit (quasi-)long-range order of any type and the superconducting and magnetic correlations which seem to diverge in the one-loop treatment remain strictly short-ranged.

As another similarity between the 2D system and the two-leg ladder we mention that also in the ladder the forward scattering amplitudes calculated within the RG scheme exhibit a  $d$ -wave-type structure with different signs for the forward scattering onto the same band and onto the other band. However a shift of the Fermi points induced by the flow of the forward scattering processes was found in a weak-coupling RG treatment only for the case of unequal Fermi velocities in the two bands [34].

Finally we add that in the 2D Hubbard model with  $t' < 0$  for band fillings  $n > 1$  corresponding to electron-doped case the situation is different from the hole-doped case described above [13]. For  $n > 1$  the  $(\pi, 0)$  and  $(0, \pi)$  regions of the BZ, that are crucial for the channel coupling leading to the combined flow in the saddle point regime similar to the two-leg ladder flow, are at larger negative band energies and exert only little influence on the low temperature physics. Correspondingly, upon moving away from half filling by increasing  $n > 1$  and suitable parameters, the flow to strong coupling rapidly changes from an AF regime with high  $T^*$  to a  $d$ -wave pairing regime with low  $T^*$  without the occurrence of an intermediate saddle point regime.

In summary, the results of the recently developed  $T$ -flow one loop RG scheme applied to the  $t$ - $t'$ - $U$  Hubbard model in 2D, are qualitatively consistent with those we found earlier using an IR-flow RG scheme. The  $T$ -flow RG scheme has the advantage that the competition with long wavelength instabilities such as a  $d$ -wave FS Pomeranchuk distortion can be analyzed in an unbiased way. Our results show that this susceptibility and also the  $d$ -density wave susceptibility are never the dominant ones in a Hubbard with just an onsite repulsion,  $U$  although for densities in the saddle point regime they appear as divergent susceptibilities together with those towards  $d$ -wave pairing and AF order. These results agree with the proposal we made earlier [12] regarding the nature of the strong coupling phase that appears at temperature  $T \leq T^*$ . Based on the close analogy with the one loop RG results for the two leg ladder at half-filling, we proposed that at  $T \approx T^*$  a crossover occurs to a strong coupling phase with a FS which is partially truncated in the vicinity of the saddle points by the formation of an insulating spin liquid which in turn is not characterized by any, even quasi, long range order. The remaining FS arcs centered on the BZ diagonals are coupled in the Cooper channel to the insulating spin liquid and this coupling is the origin of a transition to  $d$ -wave superconductivity at a lower  $T < T^*$ . Note we find that  $T^*$  is a strong function of the density and increases from zero with increasing density as the van Hove filling is crossed. This behavior of  $T^*$  is, we argue, consistent with the critical density and rising temperature scale found by Tallon and Loram [35].

Of course our one-loop approach does not yield a controlled theory of the strongly coupled phase below the characteristic temperature  $T^*$  and the second step in the weak-coupling analysis of the exemplary ladder systems, the bosonization of the effective Hamiltonian, cannot be performed in the 2D case. Thus we cannot prove the properties of the 2D strong coupling phase for the time being. More powerful methods need to be developed in order to establish the nature of the strong coupling phase at temperatures  $T < T^*$ , to test our proposal that it is closely analogous to that of the 2-leg ladder and also to examine possible connections to the gauge theories which proceed directly from strong coupling and also predict strong fluctuations coexisting in several channels such as the  $d$ -wave pairing and  $d$ -density wave channels [22].

We thank M. Sigrist, M. Troyer, D. Poilblanc, W. Metzner, and C. Nayak for helpful discussions. C.H. acknowledges support by the Swiss National Science Foundation (SNF) and the Emmy-Noether program of the Deutsche Forschungsgemeinschaft (DFG). The numerical calculations were performed on the *Asgard* Beowulf cluster of ETH Zürich.

## References

<sup>2</sup> This is also true for the 2D model restricted to the saddle point regions, see Ref. [26]

1. P.W. Anderson, *The Theory of Superconductivity in the High- $T_c$  Cuprates*, Princeton University Press (1997).

2. F. Gebhard, *The Mott Metal-Insulator Transition*, Springer Tracts in Modern Physics 137, Springer-Verlag Berlin (1997); M. Imada, A. Fujimori, Y. Tokura, Rev. Mod. Phys. **70**, 1039 (1998).
3. D. Vollhardt, N. Blümer, K. Held, and M. Kollar, cond-mat/0012203; D. Vollhardt, N. Blümer, K. Held, M. Kollar, J. Schlipf, M. Ulmke, and J. Wahle, *Advances in Solid State Physics* **38**, 383 (1999).
4. P.W. Anderson, cond-mat/0108522.
5. C.M. Varma, Z. Nussinov, and W. van Saarloos, cond-mat/0103393.
6. G. Kotliar, and J. Liu, Phys. Rev. B **38**, 5142 (1988); Y. Suzumura et al., J. Phys. Soc. Jpn. **57**, 2768 (1988); G. Baskaran, and P.W. Anderson, Phys. Rev. B **37**, 580 (1988); H. Fukuyama, Prog. Theor. Phys. **108**, Suppl., 287 (1992).
7. M. Vojta, and S. Sachdev, Phys. Rev. Lett. **83**, 3916 (1999); M. Vojta, Y. Zhang, and S. Sachdev, Phys. Rev. B **62**, 6721 (2000).
8. H.Q. Lin, and J.E. Hirsch, Phys. Rev. B **35**, 3359 (1987).
9. W. Hofstetter, and D. Vollhardt, Ann. Phys. **7**, 48 (1998).
10. D. Zanchi, and H.J. Schulz, Europhys. Lett. **44**, 235 (1997); Phys. Rev. B **61**, 13609 (2000); Europhys. Lett. **55**, 376 (2001).
11. C.J. Halboth, and W. Metzner, Phys. Rev. B **61**, 7364 (2000); Phys. Rev. Lett. **85**, 5162 (2000).
12. C. Honerkamp, M. Salmhofer, N. Furukawa and T.M. Rice, Phys. Rev. B **63**, 035109 (2001).
13. C. Honerkamp, Euro. Phys. J. B **21**, 81 (2001).
14. V.Yu. Irkhin, A.A. Katanin, and M.I. Katsnelson, Phys. Rev. B **64**, 165107 (2001).
15. B. Valenzuela and M.A.H. Vozmediano, Phys. Rev. B **63**, 153103 (2001).
16. C. Honerkamp, and M. Salmhofer, Phys. Rev. B **64**, 184516 (2001); Phys. Rev. Lett. **87**, 187004 (2001).
17. C. Nayak, Phys. Rev. B **62**, 4880 (2000).
18. S. Chakravarty, R.B. Laughlin, D.K. Morr, and C. Nayak, Phys. Rev. B **63**, 094503; S. Chakravarty, Hae-Young Kee, and C. Nayak, Int. J. Mod. Phys. B **15**, 2901 (2001).
19. I. Affleck, and J.B. Marston, Phys. Rev. B **37**, 3774 (1988).
20. H.J. Schulz, Phys. Rev. B **39**, 2940 (1989).
21. Q.H. Wang, J.H. Han, and D.H. Lee, Phys. Rev. Lett. **87**, 077004 (2001); C. Honerkamp, and M. Sigrist, J. Phys. C **13**, 11669 (2001).
22. For a recent review see P.A. Lee, cond-mat/0201052.
23. M. Salmhofer, and C. Honerkamp, Prog. Theo. Physics **105**, 1 (2001).
24. D.A. Ivanov, P.A. Lee, and Xiao-Gang Wen, Phys. Rev. Lett. **84**, 3958 (2000).
25. P.W. Leung, Phys. Rev. B **62**, R6112 (2000).
26. B. Binz, D. Baeriswyl, and B. Douçot, cond-mat/0104424.
27. N. Furukawa, M. Salmhofer, and T.M. Rice, Phys. Rev. Lett. **81**, 3195 (1998).
28. P. Frigeri, C. Honerkamp, and T.M. Rice, in preparation.
29. Y. Otsuka, Y. Morita, and Y. Hatsugai, cond-mat/0106420.
30. L. Balents, and M.P.A. Fisher, Phys. Rev. B **53**, 12133 (1996).
31. H. Lin, L. Balents, and M.P.A. Fisher, Phys. Rev. B **58**, 1794 (1998).
32. For a review, see M.P.A. Fisher, cond-mat/9806164 and references therein.
33. R.M. Noack, S.R. White, and D.J. Scalapino, Phys. Rev. Lett. **73**, 882 (1994).
34. Kim Louis, J.V. Alvarez, and C. Gros, Phys. Rev. B **64**, 113106, (2001).
35. J.L. Tallon, and J.W. Loram, Physica C **349**, 53 (2001).